VACANCIES IN HIGHLY DOPED SILICON STUDIED BY POSITRON ANNIHILATION SPECTROSCOPY

Ville Ranki

Laboratory of Physics
Helsinki University of Technology
Espoo, Finland

Dissertation for the degree of Doctor of Science in Technology to be presented with due permission of the Department of Engineering Physics and Mathematics for public examination and debate in Auditorium E at Helsinki University of Technology (Espoo, Finland) on the 1st of April, 2005, at 12 o'clock noon.

Dissertations of Laboratory of Physics, Helsinki University of Technology
ISSN 1455-1802

Dissertation 130 (2005):
Ville Ranki: Vacancies in Highly Doped Silicon Studied by Positron Annihilation Spectroscopy
ISBN 951-22-7574-0 (print)
ISBN 951-22-7575-9 (electronic)

Otamedia OY
ESPOO 2005

Abstract

Vacancy defects and their effect on electrical deactivation in highly doped silicon have been studied using positron annihilation spectroscopy. The dominant vacancy-impurity complexes are identified. The results explain the formation of compensating vacancy-impurity complexes by thermal processes during the growth. The migration kinetics leading to stable defects complexes is studied in detail with the help of electron irradiation. These results are further applied to understand the defect formation during molecular beam epitaxy under ion-implantation or low temperature growth.

In case of As doping the electron irradiation induced vacancy-arsenic pairs (V-As_1) become mobile at 450 K and migrate until stopped by substitutional As to form V-As_2 complexes. Subsequently the V-As_2 complexes start to diffuse at 700 K and create stable V-As_3 complexes by migration. The recovery of V-As_3 defects takes place after 1100 K annealing. Similar defects were observed also in P and Sb doped Si. The formation of V-As_3 defects at 700 K and their annealing at 1100 K are in perfect agreement with the well-known properties of the electrical compensation in highly doped Si.

The V-As_3 defect is also the dominant compensating vacancy defect in heavily As-doped MBE grown Si. Larger vacancy complexes, tentatively identified as V_2-As_5, are also formed at high concentrations. The V-As_3 and V_2-As_5 complexes are removed by annealings at 800 and 900°C, respectively. However, they are likely to reconstruct during the cooling down by subsequent migrations of V, V-As and V-As_2.

In highly Sb-doped Si grown by molecular beam epitaxy at low temperatures the open volume defects are neighbored by 1 – 2 Sb atoms, and their concentration is large enough to be important for the electrical deactivation. Annealing experiments show that vacancy defects are unstable already at 400 – 500 K and form larger vacancy-Sb complexes, most likely by the migration of V-Sb pairs.

The formation of thermal vacancies in highly n-type Si starts already at 700 K and at high temperatures the vacancies are mainly isolated from impurities. Upon cooling down the vacancies are quenched to stable vacancy-impurity complexes such as V-As_3 and V-P_3, which act as electrically compensating defects.

Preface

This thesis has been prepared in the Positron Group in the Laboratory of Physics at the Helsinki University of Technology during the years 2000-2005. I wish to express my gratitude to Prof. Pekka Hautojärvi for giving me the opportunity to work in this experimental group.

I am indebted to Prof. Kimmo Saarinen for excellent guidance and supervision during the time I have been in the laboratory. He has always been able to help me get forward in the work regardless of the problems encountered in designing and building the equipment, in the actual measurements and data analysis, or in understanding the results.

I wish to thank the members of the positron group, both current and former, for creating a pleasant and inspiring working environment. They have always been willing to help regardless if it's work related or simply getting the weights off my chest at the gym. Further thanks go to Prof. Martti Puska and his group for the help with the theoretical calculations. Also the help from the skillful people at the electronic and mechanical workshops is gratefully appreciated.

The financial support from the Vilho, Yrjö and Kalle Väisälä Foundation of the Finnish Academy of Science and Letters, the Emil Aaltonen Foundation and the Foundation of Technology is gratefully acknowledged.

Finally, I would like to thank my parents, my sister and her daughter Roosa for all the support and encouragement during the work of this thesis.

Espoo, March 2005

Ville Ranki

Contents

List of publications

This thesis consists of an overview and the following publications:

I V. Ranki, J. Nissilä, and K. Saarinen, *Formation of vacancy-impurity complexes by kinetic processes in highly As-doped Si*, Physical Review Letters **88**, 105506:1-4 (2002).

II V. Ranki, K. Saarinen, J. Fage-Pedersen, J. Lundsgaard Hansen, and A. Nylandsted Larsen, *Electrical deactivation by vacancy-impurity complexes in highly As-doped Si*, Physical Review B: Rapid communication **67**, 041201:1-4 (2003).

III V. Ranki, A. Pelli, and K. Saarinen, *Formation of vacancy-impurity complexes by annealing elementary vacancies introduced by electron irradiation of As-, P- and Sb-doped Si*, Physical Review B **69**, 115205:1-12 (2004).

IV M. Rummukainen, I. Makkonen, V. Ranki, M. J. Puska, K. Saarinen, and H.-J. L. Gossmann, *Vacancy-impurity complexes in highly Sb-doped Si grown by molecular beam epitaxy*, submitted to Physical Review Letters, 4 pages.

V V. Ranki and K. Saarinen, *Formation of thermal vacancies in highly As and P doped Si*, Physical Review Letters **93**, 255502:1-4 (2004).

The author has had an active role in all the phases of the research reported in this thesis. He has been involved in the planning and performing of the experiments as well as in the analysis of experimental data, and he has contributed to the interpretation of the results. The author has written Publications I, II, III and V, and helped in the preparation of Publ. IV. In addition the author had a major role in designing and implementing the automation of the measurement systems. Further, the author has perfected the data analysis software.

Chapter 1

Introduction

The computing speed of microprocessors increases due to the miniaturization of the Si field-effect transistors (FETs) which act as the basic logical elements of the device [1]. The decrease of the size of the FET requires an increase in the doping density, both at the source and drain electrodes as well as in the channel [1]. When Si is doped to concentrations above $\sim 3{\times}10^{20}$ cm^{-3} fundamental material problems start to appear. The free carrier concentration saturates to this value both in donor implanted [2] and MBE grown [3, 4] Si. As the deactivation takes place also enhanced donor diffusion is observed indicating that a new migration mechanism becomes dominant [5].

The reason for the electrical deactivation is believed to be defect complex formation, which is also related to the observed enhanced donor diffusion. One suggested group of defects are the precipitates which have been observed in Si subjected to high temperature (700 – 1000°C) annealing [2, 6, 7]. The most discussed defect complexes are however vacancy-donor complexes, where one or several Si vacancies are surrounded by one or more donor atoms at substitutional sites (V_m-D_n).

Theoretical calculations show that the formation energies of V-D_n decrease with increasing n and with $n > 2$ they become negative suggesting that defects with high n should be abundantly present at all doping levels [8, 9]. Thus also the electrical deactivation should happen at all concentrations. This is however not observed, which is usually explained by kinetic processes limiting the formation of V-D_n.

D. Mathiot and J. C. Pfister have suggested that the enhanced diffusion happens by percolation provided the donor concentration is high enough [10]. The donor atoms form an infinite cluster when they are 5th nearest neighbours or closer to each other. Then the vacancies which are 3rd nearest neighbour to a donor can

be second nearest to an another donor thus lowering the migration barrier of the donor atoms. Later it has been proposed that it is enough that the donor atoms are 9th nearest neighbours and also that larger complexes (V-D_2) can diffuse with similar mechanisms [9, 11]. The migration barrier of V-D_2 (2.0 eV for V-As_2) is however larger than for V-D_1 (1.19 eV for V-As_1) and thus migration happens only at higher temperatures [11]. Further theoretical proof for the electrical deactivation by vacancy-donor complexes has been presented by M. A. Berding and A. Sher in a form of electronic quasichemical formalism calculations which indicate that V-As_n complexes with high n are responsible for the deactivation [12].

There is also experimental evidence that vacancy-donor complexes are responsible for the observed electrical compensation and enhanced diffusion. Isoconcentration measurements by A. Nylandsted Larsen *et al.* suggest that V-Sb_1 and V-Sb_2 are responsible for the diffusion in highly Sb doped Si [13]. Theoretical calculations and extended X-ray absorption fine structure measurements (EXAFS) by K. C. Pandey *et al.* suggest that V-As_4 complex plays a strong role in the deactivation in highly As doped Si [8]. They note, however, that smaller defects, such as V-As_3, have not been considered and they can also play a role in the deactivation.

Highly doped Si has been studied with positrons earlier. D. W. Lawther *et al.* found evidence that V-As_n complexes (with average n being greater than two) are associated to the electrical deactivation in highly As doped Si [14]. U. Myler *et al.* have studied Si([As]=4×10^{20} cm^{-3}) using two detector coincidence system [15]. They observed an increase in the As signal after 500°C and 750°C annealings indicating the formation of V-As_n defects. S. Szpala *et al.* have made coincidence Doppler measurements on highly Sb-doped Si (up to 2.4×10^{21} cm^{-3}) [16]. They studied the effect of Sb to the core region of the electron momentum distribution and proposed that a single Sb bound to a vacancy is the compensating acceptor in highly doped material.

In addition to the vacancy-donor complexes other defects have been considered as well. Based on first-principles calculations and X-ray absorption measurements D. J. Chadi *et al.* have proposed a donor-pair defect as responsible for the deactivation in highly Sb doped Si [17]. These defects contain two separated but interacting dopant atoms with no associated Si vacancies. In later measurements by annular dark-field scanning transmission electron microscope by P. M. Voyles *et al.* direct evidence of Sb pairs was obtained but it was impossible to discriminate between the donor-pair and V-Sb_2 defects [18, 19].

Information related to the electrical deactivation at high doping levels have also been obtained from measurements in Si where vacancies have been created artificially by electron irradiation. By observing the defect migrations and formations in electron irradiated Si during annealings one gains information about processes taking place during the growth of Si. Since the vacancy is mobile well below

room temperature it can survive temperatures at and above room temperature only as trapped at some defect, such as at neighboring site of a donor atom. G. D. Watkins *et al.* have identified the V-D_1 defects formed by electron irradiation in P-, As- and Sb doped Si using electron paramagnetic resonance (EPR) and electron-nuclear double resonance (ENDOR) [20, 21]. They also found that these defects anneal at relatively low temperatures.

Positrons have also been applied to study electron irradiated Si. J. Mäkinen *et al.* have investigated Si([P]=10^{20} cm^{-3}) to show that positrons trap at V-P_1 defects [22, 23]. The annealing of V-D_1 defects in P, As and Sb-doped Si have been studied by A. Polity *et al.* [24]. They found that the V-D_1 defects annealed at temperatures around 400 – 450 K. They also found divacancies which annealed between 500 and 650 K. V. Avalos and S. Dannefaer have studied P and Sb doped samples with concentrations between 10^{16} and 5×10^{18} cm^{-3} [25]. Their conclusion was that at lower doping V_2-D_1 defects dominate whereas at dopings around 5×10^{18} cm^{-3} the V-D_1 is the dominant defect.

In this thesis the formation of vacancy complexes and their effect on the electrical deactivation in highly doped Si is studied using positron annihilation spectroscopy. In Publications I and III we studied the formation mechanism of electrically inactive vacancy-impurity clusters in highly n-type Si by annealing electron irradiation induced vacancy-donor pairs. Publications II and IV cover defects in as-grown and annealed samples with thin layers of very highly doped Si at the surface. Publication V discusses the important phenomenon of thermal vacancy formation in Si. In addition to the results in Si, Publication III contains some new methods for the analysis of the momentum distribution of positron-electron pair, and Chapter 3 of this thesis explains the development of positron measurement control software e^+lab.

Chapter 2

Positron annihilation experiments

Positron annihilation spectroscopy is a method that can be used to detect open volume defects and their chemical environments in a solid material. It is based on introducing positrons to a system where they eventually annihilate with electrons, their antiparticles. Before the annihilation positrons can, due to their positive charge, get trapped at neutral and negative vacancies where the Coulombic repulsion of the positive nucleus is missing. At the vacancy the electron density is lower causing the time the positron spends in the material to increase, thus allowing positron lifetime measurements to characterize the open volume of the defects. In addition the electron momentum distribution is different due to the missing atom, the relaxation of the electron cloud of the neighboring atoms and the possible impurities present next to the vacancy. Since momentum is conserved in the annihilation, the annihilation photons contain information about the electron momentum at the annihilation site. Thus the measurement of this Doppler shift can be used to obtain information about the chemical environment of the defects.

2.1 Positrons in solids

In measurements with fast positrons the positron source, commonly ^{22}Na, is sandwiched between two identical sample pieces. Thus the positrons leaving the source immediately enter the sample where they lose their energy in processes like core-electron ionization and conduction-electron and phonon scattering. This thermalization takes only a short time, but due to continuous energy distribution of the positrons, the depth distribution ends up being rather wide. Thus fast positron

measurements are best suited for samples where the region of interest is a several hundred micrometer thick homogeneous layer. After thermalization the positron diffuses in the material, possibly traps at a defect and finally annihilates with an electron.

If the layer to be studied is considerably thinner, slow positrons have to be used. In slow positron beams, the positrons from the source are directed to a moderator, such as a tungsten foil, where the positrons thermalize, and some of them escape with small energies. After discarding the fast positrons, the thermalized ones can be accelerated to desired energies with an electric field. These positrons can then be directed to the sample where their penetration depth can be adjusted by changing the accelerating electric field. The drawback of a normal slow positron beam is that in the moderation the lifetime information is lost allowing only Doppler broadening measurements. If lifetime information from a thin sample is needed, a much more complicated apparatus producing a pulsed positron beam is required.

2.2 Lifetime experiments

In positron lifetime measurements one measures the time difference between the photon created at the same time as the β-decay, 1.27 MeV photon in case of ^{22}Na, and one of the 511 keV annihilation photons. The lifetime spectrometer consists of two detectors (start and stop), both consisting of a fast scintillator coupled to a photomultiplier. The timing pulses are obtained with constant-fraction discriminators. A time-to-amplitude converter is used to obtain pulses with amplitude proportional to the time difference between the two photons. The pulses are collected into a lifetime spectrum with a multichannel analyzer. Usually about $2{\times}10^6$ events are collected to a single spectrum during a time of couple of hours.

The positron lifetime spectrum, that is, the annihilation rate at time t, is the negative derivative of the number of positrons n alive at time t,

$$-\frac{dn(t)}{dt} = \sum_{i=1}^{N+1} I_i \lambda_i e^{-\lambda_i t}, \tag{2.1}$$

where I_i is the relative intensity of lifetime component $\tau_i = 1/\lambda_i$ with $\sum_i I_i = 1$ and N is the number of positron trapping states in the sample. This is the ideal case, in practice the measured spectrum is a convolution of the ideal spectrum with the resolution function of the system. In addition positrons annihilating in the source material and the foil surrounding it also cause components to the

measured spectrum. With a defect free reference sample these source components can be determined and their effect removed. Although in case of several positron traps the decomposition becomes very difficult, the average positron lifetime

$$\tau_{ave} = \int dt\ t\Big(-\frac{dn(t)}{dt}\Big) = \sum_i I_i \tau_i \tag{2.2}$$

can tell about the presence of vacancy type defects if its value is larger than the lifetime in a defect free material.

2.3 Doppler-broadening experiments

In Doppler-broadening measurements one detects the broadening of the 511 keV annihilation line caused by the momentum of the annihilating positron-electron pair. The energy of the annihilating photon is usually measured with a high-purity Ge-detector. The signal is amplified and a digital stabilizer is used in order to remove the effect of instabilities in the measurement system. The pulses are collected to an energy histogram using a multichannel analyzer.

In order to characterize the Doppler spectrum, shape parameters S and W are defined (Fig. 2.1). The S parameter is defined as the number of pulses in the center of the peak divided by the number of total counts in the peak. The S parameter thus characterizes the annihilation with the low momentum valence electrons. Typically the S parameter is calculated at photon energies $|E_\gamma - 511\ \text{keV}| < 0.7$ keV. The W parameter is the fraction of counts in the wing region of the peak and characterizes annihilations with the high momentum core electrons. Energies used for the W parameter are usually between 2.5 keV and 4.2 keV from the peak center. Positron trapping at vacancies usually increases the S parameter and decreases the W parameter. However, impurities next to the vacancy can change this behavior as can be seen in the results of this thesis.

It is possible to lower the level of background in the Doppler spectrum and thus study even higher momentum electrons by detecting both of the annihilation photons. One way to do this is to use a second detector only for gating purpose only allowing those pulses to be added to the spectrum where both detectors have detected a photon within a certain coincidence time. The advantage of doing it this way is that the resolution of the second detector doesn't have to be very good.

Even better results can be obtained, however, by using two Ge-detectors and placing the observed signals into a two-dimensional matrix where the energies observed determine the column and row where the pulse is added (Fig. 2.1). Due to the conservation of momentum the actual annihilation events will be at the

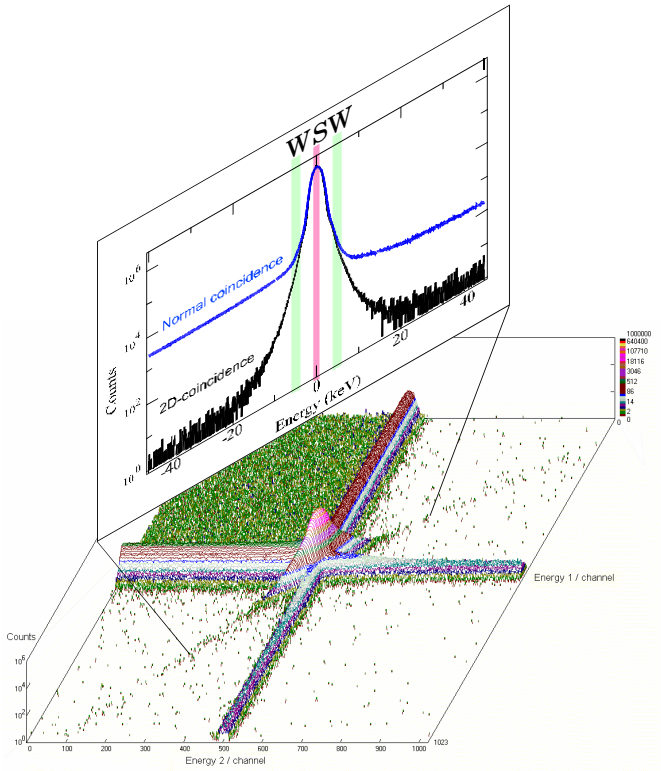

Figure 2.1: Two dimensional Doppler spectrum from coincidence measurement, normal one dimensional spectrum obtained from it and the S and W parameter windows.

diagonal of the 2D-spectrum since $E_1 + E_2 = 2m_0c - E_b$, where E_b is the binding energy of positron and electron in the solid. Due to finite resolution of the system counts where the sum of the photon energies are close to $2m_0c$ are accepted to the final 1D spectrum. In addition to the very high peak-to-background ratio the resolution is improved by a factor of $\sqrt{2}$ in this system. As an added bonus the resolution function of the system can be obtained from the other diagonal. The effect of the resolution of the measurement system can be removed from the valence region of the spectrum by deconvolution. The deconvolution can be made for example with the model-independent unfolding method [26], more details can be found in Publ. III.

2.4 Analysis of results

In the case of positron trapping at one kind of a defect the measured annihilation parameter P (S or W parameter or the average lifetime τ_{ave}) can be written as a superposition of the defect parameter P_D and the parameter of perfect lattice P_B as

$$P = \eta P_D + (1 - \eta) P_B, \tag{2.3}$$

where η is the fraction of positrons annihilating at the defect. By using the trapping rate κ_D and the positron annihilation rate from the delocalized state $\lambda_B = 1/\tau_B$, the concentration of the defects can be estimated as

$$c_D = \frac{\kappa_D N_{at}}{\mu_D} = \frac{N_{at}}{\mu_D \tau_B} \frac{(P - P_B)}{(P_D - P)}, \tag{2.4}$$

where N_{at} is the atomic density and μ_D the positron trapping coefficient. In semiconductors the temperature behavior of μ_D depends on the charge of the vacancy. For positive vacancies μ_D is small and thus trapping is usually not seen. For neutral defects the positron trapping coefficient is temperature independent with values around 10^{14} – 10^{15} s^{-1} and thus defects with concentrations above 10^{16} cm^{-3} can be detected. For negative vacancies the μ_D increases with decreasing temperature. However, with very large concentrations of negative vacancies, like in most Si samples studied in this thesis, the trapping at negative vacancies is independent of temperature due to screening effects.

The Doppler broadening experiments yield chemical information on the atoms at the positron annihilation site. Hence, it has been suggested that the Doppler broadening curves could be constructed of element-specific momentum distributions which could be recorded in reference samples [16, 27, 28]. However, it is suspicious if such superposition could always be justified, since the positron state and lattice symmetry of the reference material could be very different from those in the studied sample. On the other hand, at different vacancy-impurity complexes the trapped positron state is always very similar, and thus the recorded momentum distribution can be successfully decomposed to element-specific constituents,

$$\rho(\boldsymbol{p}) = \sum_{i=1}^{m} n_i \rho_i, \tag{2.5}$$

where m is the number of different kinds of atoms next to the vacancy, n_i is the number of ith kind of atoms and ρ_i the respective electron momentum distribution. It should be noted that the ρ_i are distributions for an atom next to a

vacancy, not that of an atom in a lattice without open volume defects where the positron wavefunction is very different. More details are given in Publ. III.

To illustrate the changes of the momentum distribution $\Gamma(\boldsymbol{p})$ we apply the conventional analysis [29] to calculate the momentum space density of states from the experimental Doppler spectrum $I(p_z)$ as

$$N(p) = 4\pi p^2 \Gamma(p) = -2p \frac{dI(p)}{dp}. \tag{2.6}$$

Although this is derived assuming an isotropic $\Gamma(\boldsymbol{p})$, the density of states in Eq. (2.6) gives illustrative information on the changes of the average electron momentum, as will be seen in Section 4.1. Furthermore, Eq. (2.6) gives a much more physical representation of changes in $\Gamma(\boldsymbol{p})$ than the more commonly used ratio or difference curves [27,28,30,31].

To support the measurements the positron lifetimes and core electron momentum distributions can be calculated theoretically for different vacancy-donor complexes. In this thesis the atomic superposition method was used in the calculations [32–36]. In addition some data calculated with the more accurate *ab initio* method was available [37], and they were seen to agree well with the atomic superposition results at momentum values higher than $15{\times}10^{-3}\ m_0c$.

Chapter 3

Control software for positron measurements

Measuring a single positron lifetime or Doppler broadening spectrum usually takes 1 – 4 hours. Almost always information is wanted at different measurement conditions, that is at different temperatures, under illumination with photons of different energies and at different positron acceleration energies in case of beam measurements. This means that from a single sample several spectra are measured, and between each measurement the conditions are changed. Thus in order for the system to be efficient, the changing of conditions, starting the measurements and storing the data need to be automated.

Earlier two different measurement softwares were used, *Datcd* [38] for fast positron measurements and *Beamlab* [39] for slow positrons. *Datcd* ran under MS-DOS and was written in Fortran. *Beamlab* ran under Microsoft Windows 3.1 and was made using National Instruments LabView 4. The idea of the current measurement system, e^+lab, was that it would run on newer operating systems (Windows NT 4.0 and newer), that it could control both fast and slow positron systems and that it could also utilize a network connection to control equipment not directly connected to the computer (Fig. 3.1).

The first version of e^+lab was written by P. Pursula [40] and it was based on Beamlab since the code could quite easily be used in newer version of LabView. I continued the development and the software was taken to routine use in one of the lifetime systems. Later the software has been updated by me and several other people including Silja Holopainen, Antti Kemppinen, Katja Pennanen and Olli Ahonen. At the time of the writing the software is in use in all the lifetime systems and slow positron beams in the laboratory, and it was also used in all the measurements of this thesis.

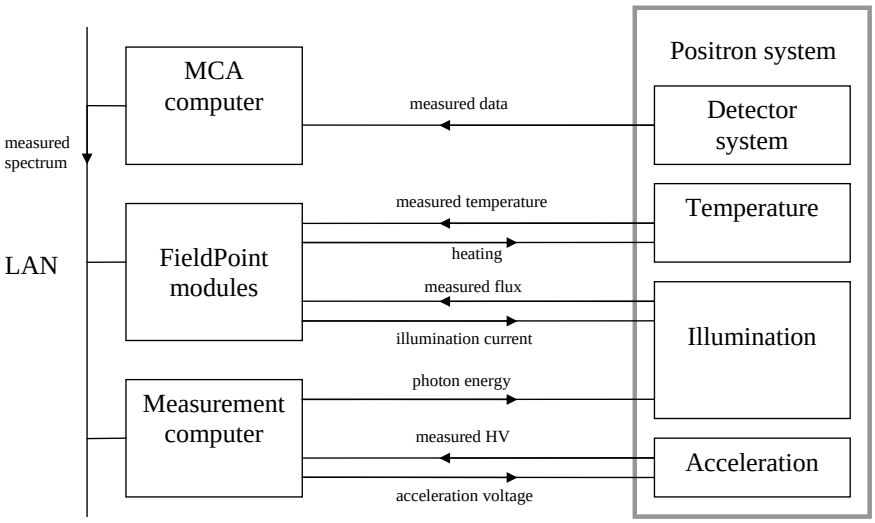

Figure 3.1: Schematic of communications between different parts of the measurement system. The measurement computer running the e^+lab software controls the FieldPoint modules and the other computer containing the multichannel analyzer.

The software can control positron lifetime measurements using both analog and digital positron spectrometers (Fig. 3.2). It can at the same time control Doppler broadening measurements with one or two detectors, including coincidence measurement. It can also fully control the temperature of the sample and the illumination system allowing different photon energies and fluxes. In case of slow positron beams the positron acceleration voltage can be controlled. Thus the system can be programmed to do measurements taking weeks without the need for user input during that time.

The system takes full use of the local area network so that none of the hardware need to be in the computer running e^+lab. The multichannel analyzer cards that are used to collect the data are located in older computers (due to the requirement of ISA-bus) needing only a network card and a small hard drive. For reading thermovoltages and controlling heating power National Instruments network-interfaced FieldPoint modules are used. For controlling positron acceleration voltage and some parts of the illumination old-fashioned serial ports are used.

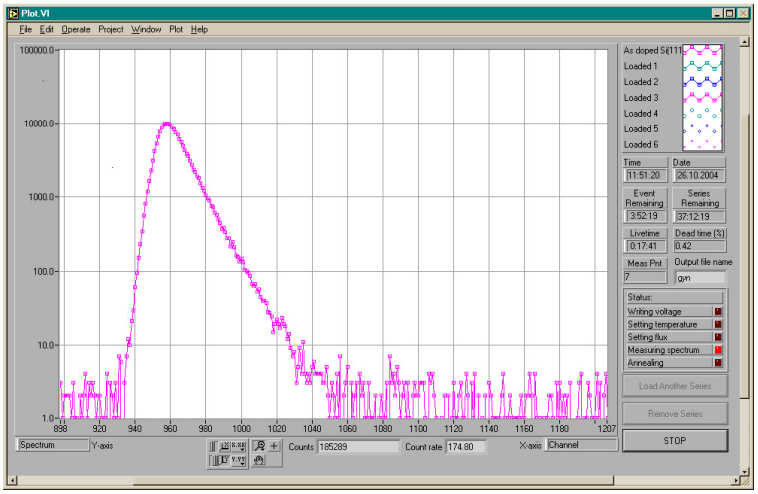

Figure 3.2: $e^{+}lab$ measurement panel during lifetime measurement.

By using external hardware moving parts of the equipment (such as monochromator used in illumination) to other systems is easier as well as the replacement of broken parts. In addition the collected data, as well as status and error logs, are also saved to a networked hard drive for easier access from different computers in the laboratory.

One of the requirements for the new system was that it should be easily configurable for different measurement systems. Thus a lot of effort was put to the numerous configuration panels allowing the tweaking of every aspect of the positron measurement system, and also the ability to quickly change between different setting collections. As an example the temperature configuration panel is shown in Fig. 3.3 including the settings for thermocouple calibration and temperature control.

During the development also the handling of different problem scenarios was taken into account, such as making sure that the heating is turned off in case of hardware or software failure. Also for most error situations, such as not reaching desired temperature in a set time or temperature fluctuating too much, the user can set the e^{+}lab to stop the measurement, give a warning or simply ignore the problem. This allows the experienced user to go beyond the set limits when testing new or malfunctioning measurement equipment.

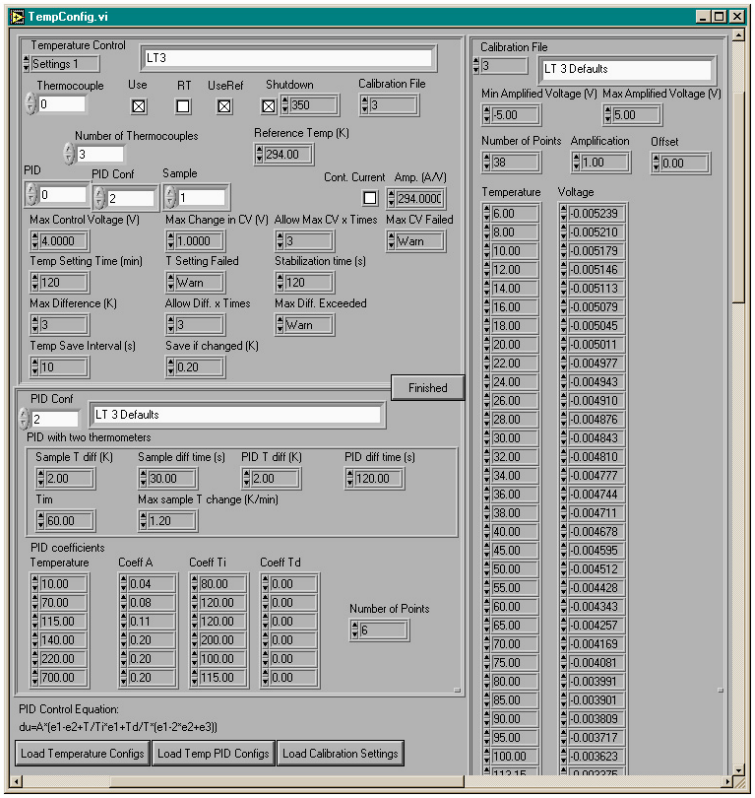

Figure 3.3: Temperature configuration panel of $e^{+}lab$.

Chapter 4

Vacancies in highly doped silicon

4.1 Measurements on electron irradiated Si

Doping levels up to 10^{20} cm^{-3} are used in current device technologies. In n-type doping of Si with arsenic, however, fundamental material problems start to appear when doping increases above $\sim 3 \times 10^{20}$ cm^{-3} [41,42]. The concentration of free electrons does not increase linearly with the doping concentration, indicating that inactive impurity clusters or compensating defects are formed. Furthermore, the diffusion coefficient of As starts to increase rapidly at [As] $> 3 \times 10^{20}$ cm^{-3} demonstrating that new migration mechanisms become dominant [5].

Both the electrical deactivation of dopants and the enhanced As diffusion have often been attributed to the formation of vacancy-impurity complexes [42]. According to theoretical calculations vacancies surrounded by several As atoms (V-As$_n$, n > 2) have negative formation energies suggesting that these complexes are abundantly present at any doping level [8,9]. The formation of these defects is, however, limited by kinetic processes such as the migration of As. At very high doping concentrations ($> 10^{20}$ cm^{-3}) the diffusion of V-As pairs is enhanced by another As at the fifth neighbor site or closer (the vacancy percolation model) [5, 10]. The calculations predict that also the V-As$_2$ complex is mobile at relatively low temperatures enabling the formation of higher order V-As$_n$ complexes [9, 11]. In fact, vacancy complexes have been observed in positron annihilation experiments [14] and recently their dominant structure has been identified as V-As$_3$ in Czochralski (Cz) Si doped up to [As] = 10^{20} cm^{-3} [30].

In Publ. I and III we applied positron annihilation spectroscopy to verify experimentally the formation mechanism of V-As$_3$ complexes in highly As doped Si, and also the formation of similar defects in P and Sb doped Si. We studied

several Czochralski-grown Si(111) bulk crystals with different As, P and Sb doping concentrations. Most of the samples were irradiated at 300 K with 2 MeV electrons in order to create vacancy defects above thermal equilibrium concentration. After electron irradiation the samples were annealed isochronally (30 min) in vacuum (10^{-3} mbar) at 300 – 1220 K, and positron lifetime measurements were conducted at room temperature between the annealings. When there were significant changes in the positron lifetime we performed coincidence Doppler broadening measurements with two Ge detectors at room temperature.

The average positron lifetime as a function of annealing temperature for samples Si([As]=10^{20} cm^{-3}) and Si([As]=10^{19} cm^{-3}) is shown in Fig. 4.1. In the Si([As]=10^{20} cm^{-3}) the lifetime is around 242 ps up to 1100 K indicating the presence of monovacancies. The peak at 500 K is due to the formation and annealing of divacancy defects. In the less doped sample the lifetime decreases in a wide temperature range indicating that the vacancy concentration is decreasing.

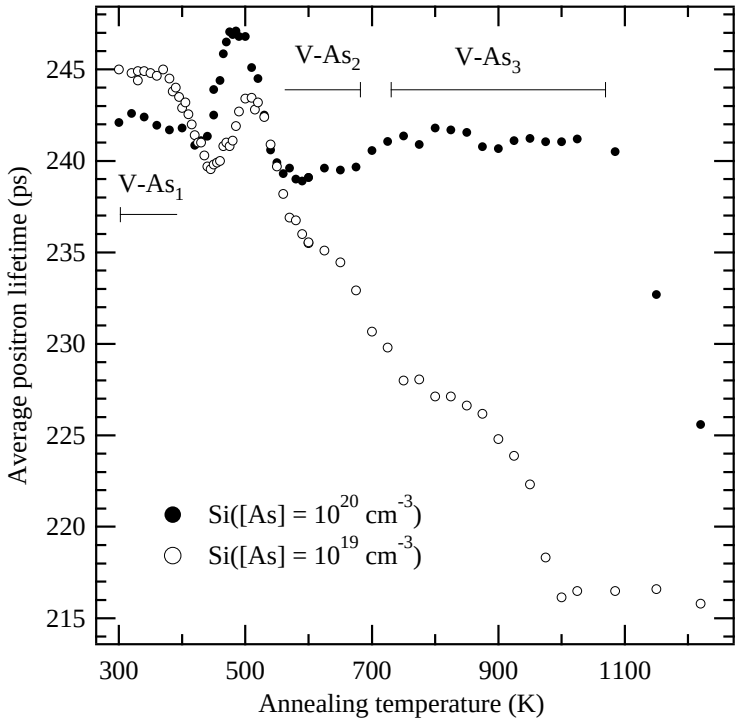

Figure 4.1: Average positron lifetime as a function of annealing temperature for electron irradiated samples Si([As]=10^{19} cm^{-3}) and Si([As]=10^{20} cm^{-3}).

In Fig. 4.2 the core region electron momentum distribution from sample Si([As]=10^{20} cm^{-3}) is shown at several temperatures. It is seen that the spectrum rises from the as-irradiated case as temperature increases. This increase is caused

by increased positron annihilation with the As 3d electrons indicating that the number of As atoms next to vacancy increases. With the help of theoretical calculations the defects can be identified as V-As_1 in as-irradiated, V-As_2 at 600 K and V-As_3 at 775 K. Furthermore, the defects in the as-grown sample are the same V-As_3 defects as after irradiation and annealing, although their concentration is much smaller. In the lower part of Fig. 4.2 the element-specific contributions (see Sect. 2.4) of Si and As atoms to the momentum distribution are shown from both measurements and theoretical calculations [37]. The agreement of measurements with theory is excellent.

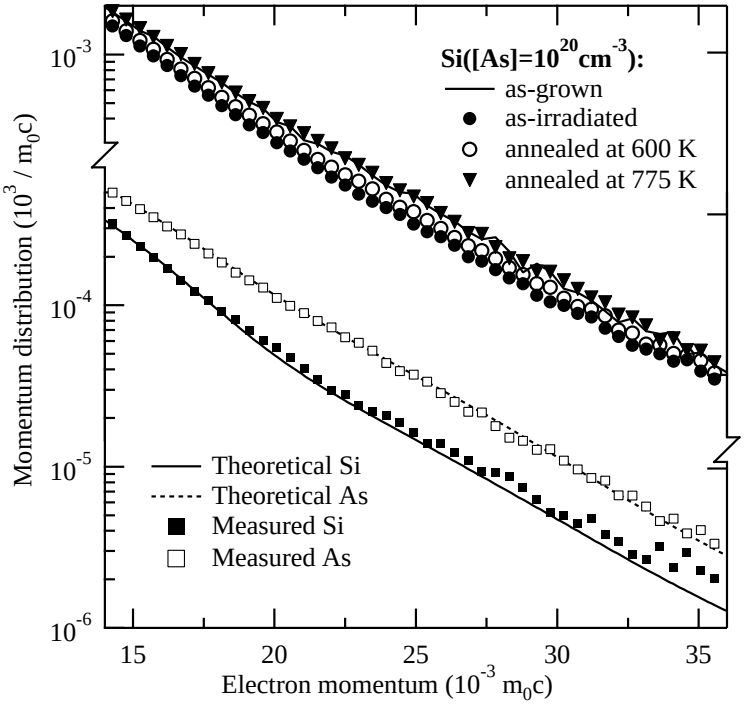

Figure 4.2: Core region momentum distributions measured in sample Si([As]=10^{20} cm^{-3}). In the as-grown sample we have removed the effect from delocalized positrons with the help of measured positron lifetimes. Below are shown the element specific momentum distributions. The theoretical calculations are from Ref. [37].

Fig. 4.3 shows the valence region electron momentum distributions from sample Si([As]=10^{20} cm^{-3}), and also the densities of momentum states (Eq. 2.6) are shown. The shift of the spectra to higher momentum at higher temperatures allows the identification of the defects also from the valence region spectra. The reason of this shift is an increase of As atoms near vacancies at higher tempera-

tures; valence electron density and also the electron momentum near the As atom is higher than near Si due to the positive charge of the As ion.

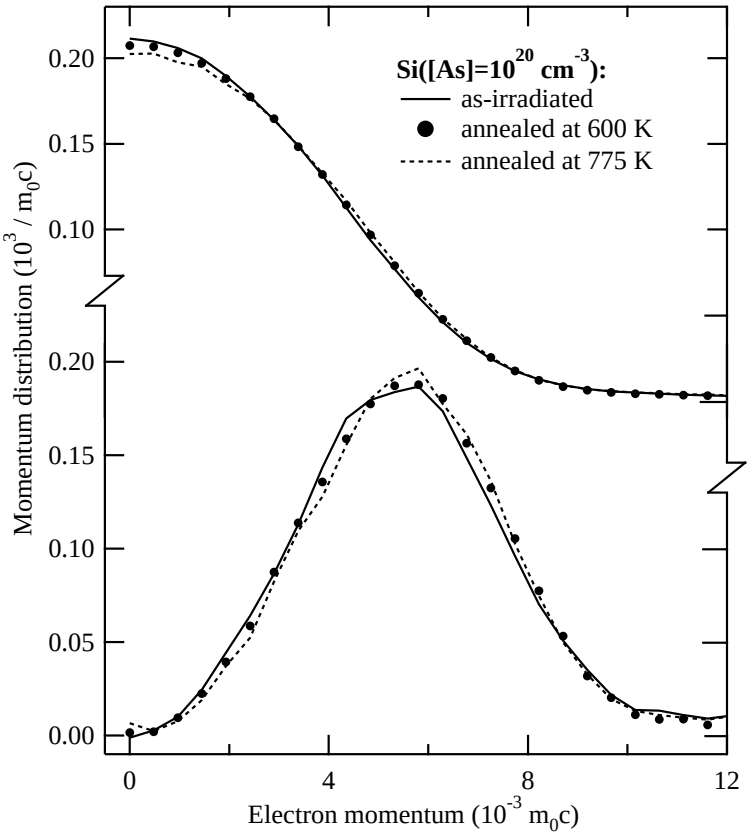

Figure 4.3: Deconvoluted valence region momentum distributions measured in sample Si([As]=10^{20} cm^{-3}). Also shown are densities of momentum spaces (lower part of the figure).

Similar complexing of donor atoms next to the vacancy at increased temperatures is also seen in P and Sb doped samples. Although the core region electron momentum distribution can't be used to identify the defects in P doped sample (also in case of Sb it is difficult), the valence region spectra show similar shift to higher momentum as in the case of As doping.

4.2 Annealings of highly As doped as-grown Si

Vacancies surrounded by three As atoms, V-As_3, have been identified in Czochralski (Cz) grown bulk Si doped up to [As]=10^{20} cm^{-3} and their formation has been explained by kinetic migration processes in Publ. I and III and in Refs. [9,11,30]. However, the concentration of V-As_3 complexes in Cz Si([As]=10^{20} cm^{-3}) is only 0.1 % of the As concentration [30] and the material does not show substantial electrical deactivation. Furthermore, it has been suggested that pairs of dopant atoms without vacancies are dominant at high doping levels [17,18]. It is thus interesting to study the structure of compensating defect complexes at [As] $> 10^{20}$ cm^{-3} where the electrical deactivation of doping becomes substantial. Equally important is to understand what happens to defect complexes in rapid thermal annealing (RTA) treatments which are routinely used to activate the doping after the growth.

In Publ. II we studied silicon samples with 330 nm thin MBE grown epitaxial layers doped heavily with arsenic (1.5×10^{20} and 3.5×10^{20} cm^{-3}). The epitaxial layers were grown on p-type, 80 Ω-cm, (001)-oriented Si float-zone refined substrates kept at a temperature of 450°C during the growth. The growth rate was 0.02 nm/s and the As ions were implanted at an energy of 1 keV during the growth. The samples were subjected to annealing in N_2, either with RTA at 900°C for 10-170 s or furnace annealing at 800-900°C for two minutes.

The electrical activities in the samples were deduced from Hall effect/resistivity measurements and the total As concentrations were determined with Rutherford backscattering spectrometry (RBS) using 2-MeV alpha particles. Doppler broadening measurements with a slow positron beam were conducted to identify the defects in the samples and estimate their concentrations.

In Fig. 4.4 S and W parameters measured from the highly doped layers in the samples after different heat treatments are shown. All the points fall on a line not going through the point characterizing the defect free lattice. There are thus at least two different positron trapping defects in the samples. Based on results in Publ. I and III the defects on the left side of the plot can be identified as V-As_3. The higher S parameter and similar W parameter shows that the defects on the right side are most likely divacancies with several As atoms as nearest neighbors, tentatively identified here as V_2-As_5 defects.

Based on the electrical and positron measurements the concentrations of the defects can be approximated. The electrical activities and the obtained defect concentrations are shown in Table 4.1. These results allow us to propose that defect reactions shown in Fig. 4.5 take place in highly As doped Si during annealing and cooling down.

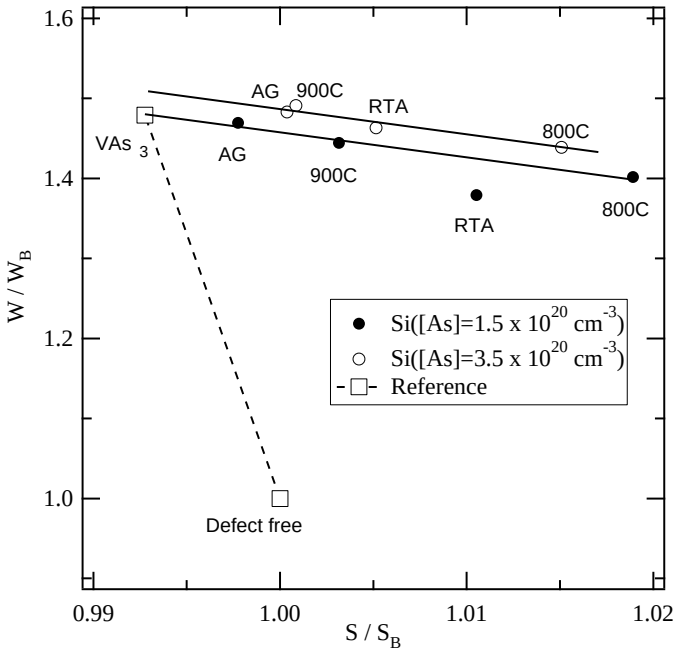

Figure 4.4: Relative W parameters (20 – $25{\times}10^{-3}$ m_0c) as function of relative S parameters (0 – $3{\times}10^{-3}$ m_0c) from all the measured samples and a sample containing V-As_3 defects. All measurements were made with the 2-parameter system and the spectra were deconvoluted before the calculation of S parameter. AG in the plot denotes as-grown and RTA rapid thermal annealed samples.

The results show that a vacancy surrounded by three As atoms is the dominant compensating vacancy defect in heavily As-doped MBE grown Si. Larger vacancy complexes, tentatively identified as V_2-As_5, are also formed at high concentrations. The V-As_3 and V_2-As_5 complexes are removed by annealings at 800 and 900°C, respectively. However, they are likely to reconstruct during the cooling down by subsequent migrations of V, V-As and V-As_2. The rapid thermal annealing is shown to lead to smallest concentrations of V-As_3 and V_2-As_5 complexes, most likely due to the limited time available for the migration processes.

4.3 Annealings of highly Sb doped as-grown material

The molecular beam epitaxy (MBE) growth at low temperature ($<$ 600 K) can be applied to achieve metastable doping and free electron concentrations which become compensated only at 10^{21} cm^{-3} [3]. At these very high doping levels the pairing of impurities may happen due to purely statistical reasons [17, 18].

Table 4.1: Arsenic concentrations and electrical activities of the measured samples. The concentrations of V-As_3 and V_2-As_5 defects were obtained by combining the results of electrical and positron experiments.

[As] 10^{20} cm^{-3}	Treatment	el. act. %	[VAs_3] 10^{18} cm^{-3}	[V_2As_5] 10^{18} cm^{-3}
1.5	as-grown	20	31 ± 3	5 ± 2
1.5	furnace at 800°C	74	2 ± 2	6 ± 2
1.5	furnace at 900°C	79	6 ± 1	0.26 ± 0.06
1.5	RTA at 800°C	88		
1.5	RTA at 900°C	98	0.4 ± 0.2	0.38 ± 0.08
3.5	as-grown	2	80 ± 9	20 ± 5
3.5	furnace at 800°C	54	1.4 ± 0.8	24 ± 5
3.5	furnace at 900°C	63	28 ± 4	9 ± 3
3.5	RTA at 800°C	67		
3.5	RTA at 900°C	85	9 ± 2	5 ± 2

The electron microscopy studies have indeed observed donor pairs at concentrations expected for compensating defects [18, 19]. These pairs (DP) have been recently attributed to the configuration DP-V-I, where the Si atom neighboring the Sb dopant pair has relaxed toward the interstitial site (I) leaving a vacancy (V) behind [19]. The presence and size of open volume in this defect has been deduced indirectly by comparing the positions of the Sb atoms to the theoretically predicted lattice relaxation [19]. On the other hand, the positron annihilation experiments of Szpala et al. suggest that open volume defects larger than monovacancies may be present [16].

In Publ. IV we applied positron annihilation spectroscopy to study vacancies formed in the low-temperature (550 K) MBE growth of highly Sb-doped Si(100). Four samples were studied with concentrations ranging from 2.7×10^{19} cm^{-3} to 3.7×10^{21} cm^{-3}. These were the same samples used in the electron microscopy experiments in Refs. [18, 19]. The Sb-doped Si(111) samples (same as in Publ. III) were used as reference.

Since the doped layer was very thin (30 – 70 nm), all measurements were made with a slow positron beam. Fig. 4.6 shows the relative S parameter as a function of positron implantation energy. The high peak in the most heavily doped sample shows that vacancies much larger than monovacancies are present in the sample indicating heavy damage. In the two least doped samples no clear peak is observed, whereas in the sample with second highest doping ([Sb]=9.4×10^{20} cm^{-3}) the S parameter shows the presence of vacancy type defects.

In order to identify the defects in the [Sb]=9.4×10^{20} cm^{-3} sample coincidence

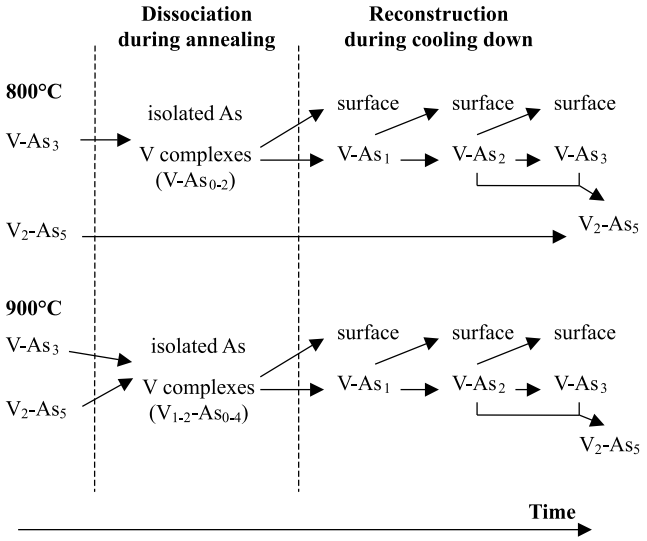

Figure 4.5: Effect of annealing in highly As-doped Si.

Doppler broadening measurement were made. By comparing the spectra with the reference samples and with theoretical calculations it was seen that that the defects are mostly mono- and divacancies with 1-2 Sb atoms as nearest neighbour. The results are in agreement with the microscopy studies [18] where Sb impurities appear either isolated or in pairs. However, no evidence of the donor pair defects were found.

The thermal stability of vacancies is studied in Fig. 4.7. While the S parameter is almost constant during annealings at 300 – 600 K, the W parameter increases significantly. These results and coincidence measurements show that the mono- and divacancies after 600 K heat treatment are neighbored by 2 – 3 Sb atoms. We attribute this to the clustering induced by the V-Sb pair, which becomes mobile at 400 – 500 K. The highly Sb-doped MBE Si is thus atomically metastable after the growth; the grown-in vacancies mediate the formation of larger vacancy-Sb clusters by annealing already below the growth temperature. The concentration of the vacancies can be approximated to be order of 10^{20} cm^{-3} and thus it is large enough to be important in the electrical deactivation of the Sb doping.

4.4 Formation of thermal vacancies

The vacancies formed in thermal equilibrium in Si are important, since they mediate the diffusion of both lattice and impurity atoms. Their role is also prominent

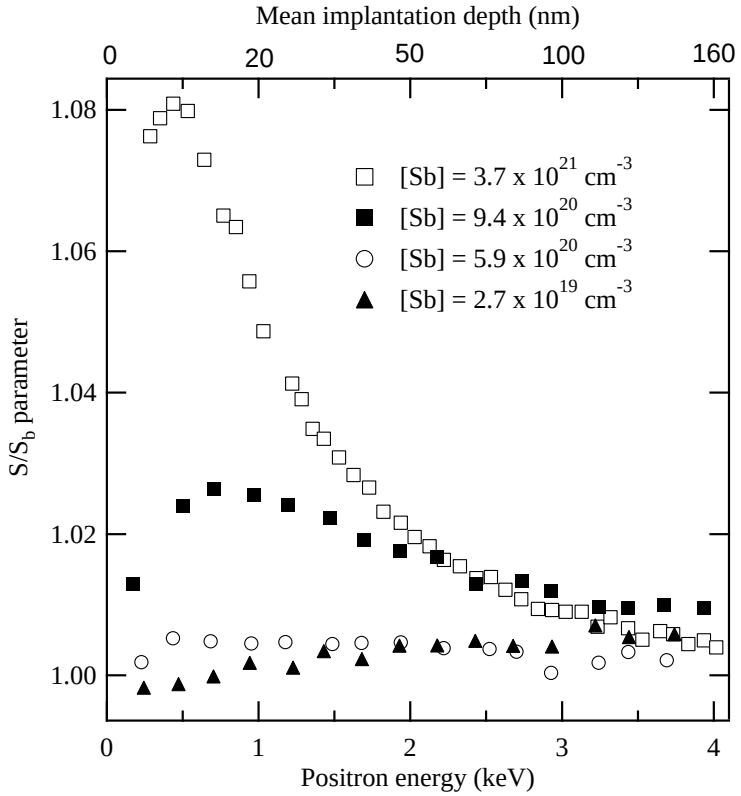

Figure 4.6: S parameter as a function of positron implantation energy. The S parameter is scaled to the bulk lattice value S_B obtained in the substrate.

in the electrical properties of highly-doped material, since the vacancy diffusion leads to the formation of electrically passive donor impurity clusters. However, the thermal vacancies have escaped the direct experimental observation and thus their basic thermodynamical properties have been uncertain.

In Publ. V we studied several Czochralski-grown Si(111) bulk crystals with As and P dopings of 10^{20} cm^{-3}. The as-grown Si([As]=10^{20} cm^{-3}) sample contains a small concentration ($\sim 10^{17}$ cm^{-3}) of native V-As$_3$ defects [30]. In the as-grown Si([P]=10^{20} cm^{-3}) sample the vacancy concentration was less than 10^{16} cm^{-3} [30]. We performed both isochronal and isothermal annealings, during which the samples were kept in a vacuum of 10^{-3} mbar, in order to study the formation of thermal vacancies.

The average lifetimes measured from the Si([As]=10^{20} cm^{-3}) and Si([P]=10^{20} cm^{-3}) samples are shown in Fig. 4.8 as a function of isochronal (30 min) annealing temperature. Between each annealing positron lifetime was

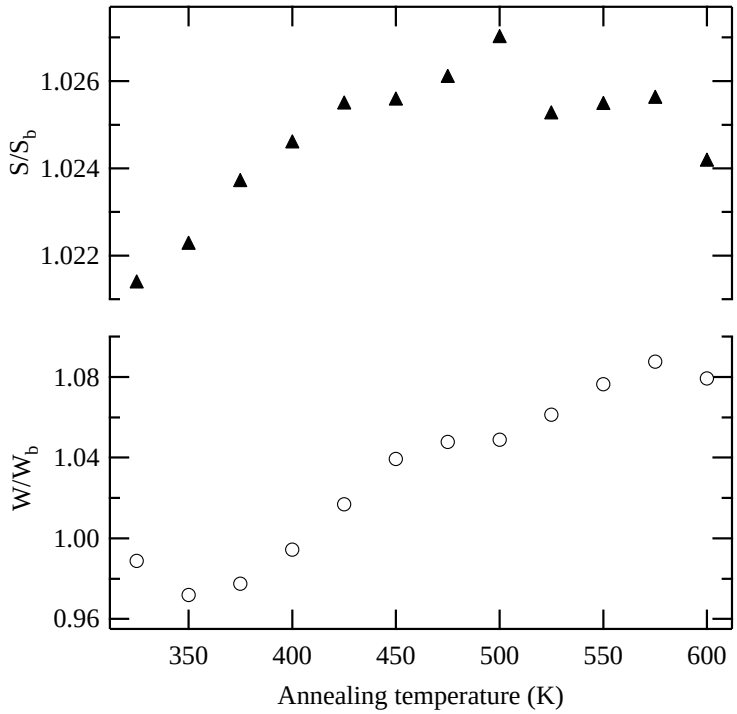

Figure 4.7: S and W parameter as a function of annealing temperature measured in Si([Sb]=9.4×10^{20} cm^{-3}) at 300 K. The parameters are scaled to the defect free lattice values S_B and W_B.

measured at room temperature. The average lifetime start to increase at 800 K and 900 K in P and As doped samples, respectively, indicating that vacancy type defects are formed. By performing the Doppler broadening experiments similarly as in Publ. I – III, we can identify the defects in Si([As]=10^{20} cm^{-3}) as V-As$_3$. The results of Fig. 4.8 thus show that thermal vacancies are formed above 900 K and they are quenched to vacancy-impurity complexes during the annealing and cooling down.

In order to observe the thermal vacancy directly we performed positron lifetime experiments during the annealing at the equilibrium temperature. The increase of the average lifetime shows that the vacancies start to form already at 650 K. With the help of these equilibrium measurements and similar measurements with a slow positron beam we can get estimates for the concentrations of these thermally generated defects. The results are shown in Fig. 4.9. With the help of the data in the figure and by using a diffusion equation we can get estimates for vacancy formation and migration energies, E_f = 1.1(2) eV and E_m = 1.2(1) eV. The low value of E_f can be explained by vacancy formation next to dopant atoms,

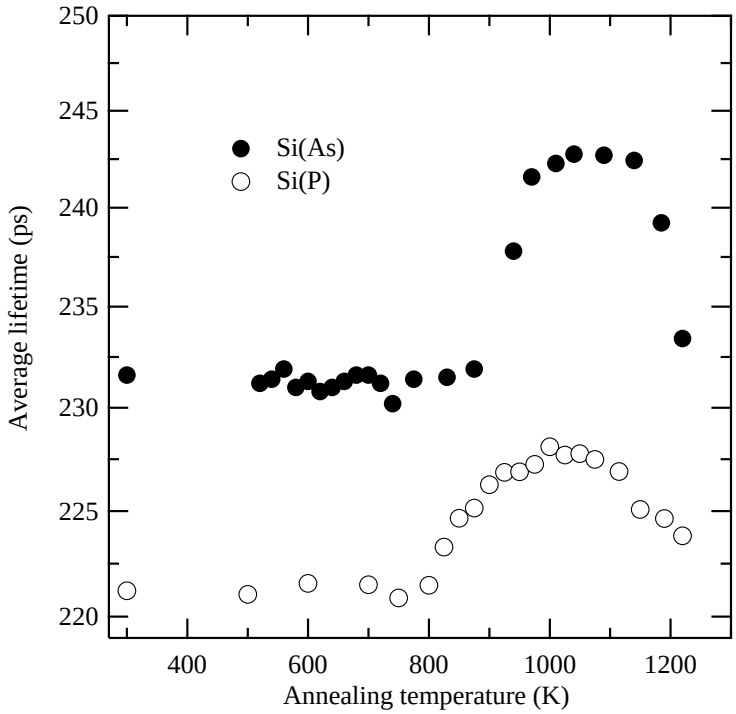

Figure 4.8: Average positron lifetime as a function of annealing temperature. The annealing time at each point was 30 minutes and the measurements were made at 300K.

resulting in an energy gain due to attractive binding. Taking the vacancy-impurity interaction into account we can estimate a formation energy of 2.8(3) eV for the neutral monovacancy in intrinsic Si.

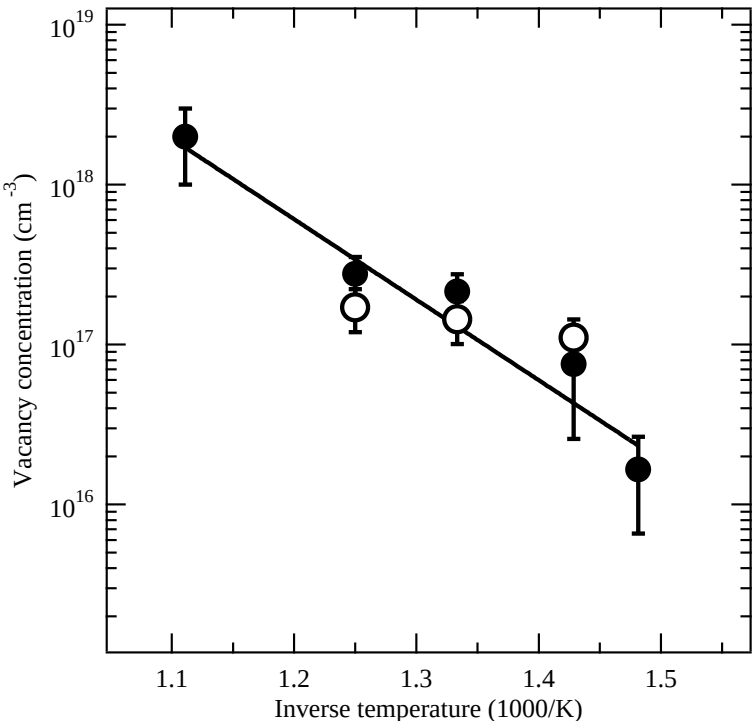

Figure 4.9: Concentration of thermal vacancies as a function of inverse temperature. The results have been obtained with lifetime experiments (filled symbols) and Doppler broadening measurements with slow positron beam (open symbols).

Chapter 5

Summary

In this thesis vacancy type defects and their contribution to the electrical deactivation of highly n-type silicon was studied. In Publ. I and III we studied the annealing behavior of vacancy-donor pair (V-D_1) created by electron irradiation. In case of As doping the V-As_1 pairs become mobile at 450 K (activation energy 1.3(2) eV) and migrate until stopped by substitutional As to form V-As_2 complexes. Subsequently the V-As_2 complexes start to diffuse at 700 K and create stable V-As_3 complexes by migration (activation energy 2.0(2) eV). These processes manifest the formation of higher-order vacancy-impurity clusters by the ring diffusion mechanism. In Publ. III it was seen that similar processes take place also in P and Sb doped Si.

We further observed the recovery of V-As_3 defects after 1100 K annealing. The formation of V-D_3 defects at 700 K and their annealing at 1100 K are in perfect agreement with the well-known properties of the electrical compensation in highly doped Si. The observed decrease of free electron concentration after heat treatment at 700 – 800 K and subsequent reactivation of doping at 1100 – 1300 K can thus be explained by the formation and annealing of the V-D_3 defects.

In Publ. II we have shown that the V-As_3 defect is also the dominant compensating vacancy defect in heavily As-doped MBE grown Si. Larger vacancy complexes, tentatively identified as V_2-As_5, are also formed at high concentrations. The V-As_3 and V_2-As_5 complexes are removed by annealings at 800 and 900°C, respectively. However, they are likely to reconstruct during the cooling down by subsequent migrations of V, V-As and V-As_2. The rapid thermal annealing, as opposed to furnace annealing, is shown to lead to smallest concentrations of V-As_3 and V_2-As_5 complexes, most likely due to the limited time available for the migration processes.

In Publ. IV we studied the vacancies in highly Sb-doped Si grown by molecular

beam epitaxy at low temperatures. The open volume defects are neighbored by 1 – 2 Sb atoms, and their concentration is large enough to be important for the electrical deactivation of Sb doping. Annealing experiments show that vacancy defects are unstable already at 400 – 500 K and form larger vacancy-Sb complexes, most likely by the migration of V-Sb pairs. The results demonstrate the metastable nature of Sb doping in Si grown by low-temperature MBE and explain the high electrical activation of Sb and deactivation in annealing by kinetic migration processes of vacancy defects.

The formation of thermal vacancies in highly P and As doped Si was studied in Publ. V. It was observed that the formation starts already at 700 K and at high temperatures the vacancies are mainly isolated from impurities. Upon cooling down the vacancies are quenched to stable vacancy-impurity complexes such as V-As_3 and V-P_3, which act as electrically compensating defects. The vacancy formation and migration energies are estimated as $E_f = 1.1(2)$ eV and $E_m = 1.2(1)$ eV, respectively. The low value of E_f can be explained by vacancy formation next to the dopant atoms, resulting in an energy gain due to attractive binding. Taking the vacancy-impurity interaction into account we can estimate a formation energy of 2.8(3) eV for the neutral monovacancy in intrinsic Si.

In addition to the results in highly doped Si the measurement control software e^+lab was developed and is now in routine use in all the positron systems at Laboratory of Physics. Also some improvements were made to data analysis software, and some new methods, such as element specific momentum distributions, were tested.

Bibliography

[1] P. A. Packan, Science **285**, 2079 (1999).

[2] A. Nylandsted Larsen, F. T. Pedersen, G. Weyer, R. Galloni, R. Rizzoli, and A. Armigliato, J. Appl. Phys. **59**, 1908 (1986).

[3] H.-J. Gossmann, F. C. Unterwald, and H. S. Luftman, J. Appl. Phys. **73**, 8237 (1993).

[4] H. H. Radamson, J. M. R. Sardela, L. Hultman, and G. V. Hansson, J. Appl. Phys. **76**, 763 (1994).

[5] A. Nylandsted Larsen, K. K. Larsen, and P. E. Andersen, J. Appl. Phys. **73**, 691 (1993).

[6] J. L. Allain, J. R. Regnard, A. Bourret, A. Parisini, A. Armigliato, G. Tourillon, and S. Pizzini, Phys. Rev. B **46**, 9434 (1992).

[7] C. Revenant-Brizard, J. R. Regnard, S. Solmi, A. Armigliato, S. Valmorri, C. Cellini, and F. Romanato, J. Appl. Phys. **79**, 9037 (1996).

[8] K. C. Pandey, A. Erbil, I. G. S. Cargill, R. F. Boehme, and D. Vanderbilt, Phys. Rev. Lett. **61**, 1282 (1988).

[9] M. Ramamoorthy and S. T. Pantelides, Phys. Rev. Lett. **76**, 4753 (1996).

[10] D. Mathiot and J. C. Pfister, J. Appl. Phys. **66**, 970 (1989).

[11] J. Xie and S. P. Chen, Phys. Rev. Lett. **83**, 1795 (1999).

[12] M. A. Berding, A. Sher, M. van Schilfgaarde, P. M. Rousseau, and W. E. Spicer, Appl. Phys. Lett. **72**, 1492 (1998).

[13] A. Nylandsted Larsen, P. Kringhøj, J. Lundsgaard Hansen, and S. Yu. Shiryaev, J. Appl. Phys. **81**, 2173 (1997).

[14] D. W. Lawther, U. Myler, P. J. Simpson, P. M. Rousseau, P. B. Griffin, and J. D. Plummer, Appl. Phys. Lett. **67**, 3575 (1995).

[15] U. Myler, R. D. Goldberg, A. P. Knights, D. W. Lawther, and P. J. Simpson, Appl. Phys. Lett. **69**, 3333 (1996).

[16] S. Szpala, P. Asoka-Kumar, B. Nielsen, J. P. Peng, S. Hayakawa, K. G. Lynn, and H.-J. Gossmann, Phys. Rev. B **54**, 4722 (1996).

[17] D. J. Chadi, P. H. Citrin, C. H. Park, D. L. Adler, M. A. Marcus, and H.-J. Gossmann, Phys. Rev. Lett. **79**, 4834 (1997).

[18] P. M. Voyles, D. A. Muller, J. L. Grazul, P. H. Citrin, and H.-J. L. Gossmann, Nature **416**, 826 (2002).

[19] P. M. Voyles, D. J. Chadi, P. H. Citrin, D. A. Muller, J. L. Grazul, P. A. Northrup, and H.-J. L. Gossmann, Phys. Rev. Lett. **91**, 125505 (2003).

[20] G. D. Watkins and J. W. Corbett, Phys. Rev. **134**, A1359 (1964).

[21] E. L. Elkin and G. D. Watkins, Phys. Rev. **174**, 881 (1968).

[22] J. Mäkinen, C. Corbel, P. Hautojärvi, P. Moser, and F. Pierre, Phys. Rev. B **39**, 10162 (1989).

[23] J. Mäkinen, P. Hautojärvi, and C. Corbel, J. Phys.: Condens. Matter **4**, 5137 (1992).

[24] A. Polity, F. Börner, S. Huth, S. Eichler, and R. Krause-Rehberg, Phys. Rev. B **58**, 10363 (1998).

[25] V. Avalos and S. Dannefaer, Phys. Rev. B **58**, 1331 (1998).

[26] K. Shizuma, Nucl. Instr. and Meth. **150**, 447 (1978).

[27] P. Asoka-Kumar, M. Alatalo, V. J. Ghosh, A. C. Kruseman, B. Nielsen, and K. G. Lynn, Phys. Rev. Lett. **77**, 2097 (1996).

[28] M. Biasini, G. Ferro, P. Folegati, and G. Riontino, Phys. Rev. B **63**, 092202 (2001).

[29] A. T. Stewart, Can. J. Phys. **35**, 168 (1957).

[30] K. Saarinen, J. Nissilä, H. Kauppinen, M. Hakala, M. J. Puska, P. Hautojärvi, and C. Corbel, Phys. Rev. Lett. **82**, 1883 (1999).

[31] R. Krause-Rehberg and H. S. Leipner, *Positron Annihilation in Semiconductors* (Springer, Berlin, 1999).

[32] M. Alatalo, H. Kauppinen, K. Saarinen, M. J. Puska, J. Mäkinen, P. Hautojärvi, and R. M. Nieminen, Phys. Rev. B **51**, 4176 (1995).

[33] M. Alatalo, B. Barbiellini, M. Hakala, H. Kauppinen, T. Korhonen, M. J. Puska, K. Saarinen, P. Hautojärvi, and R. M. Nieminen, Phys. Rev. B **54**, 2397 (1996).

[34] B. Barbiellini, M. J. Puska, T. Torsti, and R. Nieminen, Phys. Rev. B **51**, 7341 (1995).

[35] B. Barbiellini, M. J. Puska, T. Korhonen, A. Harju, T. Torsti, and R. Nieminen, Phys. Rev. B **53**, 16201 (1996).

[36] M. J. Puska and R. M. Nieminen, J. Phys. F **13**, 2695 (1983).

[37] M. Hakala, M. J. Puska, and R. M. Nieminen, Phys. Rev. B **57**, 7621 (1998).

[38] H. Kauppinen, Master's thesis, Helsinki University of Technology, 1993.

[39] J. Hassel, Beamlab-mittausohjelma hitaiden positronien suihkuun, Special assignment at Helsinki University of Technology (1997).

[40] P. Pursula, e+lab -mittausohjelmisto positronispektroskopiaan, Special assignment at Helsinki University of Technology (2000).

[41] A. Lietoila, J. F. Gibbons, and T. W. Sigmon, Appl. Phys. Lett. **36**, 765 (1980).

[42] P. M. Fahey, P. Griffin, and J. D. Plummer, Rev. Mod. Phys. **61**, 289 (1989).